Impact of the geometry of resonant magnetic perturbations on the dynamics of transport barrier relaxations at the tokamak edge

P. Beyer 1,2), F. de Solminihac 1,2), M. Leconte 3), X. Garbet 4), S. Benkadda 1,2)

1) France-Japan Magnetic Fusion Laboratory, LIA 336 CNRS, Marseille, France
2) International Institute for Fusion Science, Université de Provence, Marseille, France
3) Universite Libre de Bruxelles, Brussels, Belgium
4) CEA, IRFM, F–13108 Saint Paul Lez Durance, France

E-mail contact of main author: peter.beyer@univ-provence.fr

Abstract. The control of transport barrier relaxation oscillations by resonant magnetic perturbations (RMPs) is investigated with three-dimensional turbulence simulations of the tokamak edge. It is shown that single harmonics RMPs (single magnetic island chains) stabilize barrier relaxations. In contrast to the control by multiple harmonics RMPs, these perturbations always lead to a degradation of the energy confinement. The convective energy flux associated with the non-axisymmetric plasma equilibrium in presence of magnetic islands is found to play a key role in the erosion of the transport barrier that leads to the stabilization of the relaxations.

1. Introduction

Transport barriers in tokamak plasmas are key ingredients of improved confinement regimes. These barriers are thin layers in which turbulent transport of heat and matter is reduced significantly and a strong pressure gradient builds up. At the plasma edge, the barrier typically is not stable but exhibits relaxation oscillations associated with intermittent high energy flux peaks. These barrier relaxations are an essential characteristics of the so called edge localized modes (ELMs) [1]. The control of such ELMs is a crucial issue for the next generation of tokamak experiments such as ITER. Experimental studies on a variety of different tokamaks such as DIII-D [2, 3], JET [4], and TEXTOR [5, 6] reveal that a qualitative control of ELMs can be obtained by imposing resonant magnetic perturbations (RMPs) at the plasma edge. Such a perturbation has the same helicity as the magnetic field line on a particular (resonant) magnetic surface, and leads to a perturbation of this surface by the formation of magnetic islands [7].

The control of ELMs by RMPs is generally attributed to a reduction of the pressure gradient by a radial energy flux associated with the strong collisional heat flux along perturbed field lines [8]. In particular, it has been found that when increasing the perturbation amplitude, ELMs control becomes efficient when field line stochasticity appears, induced by overlapping magnetic islands [8]. However, the actual amplitude of the magnetic perturbation inside the plasma is not precisely known yet, as the penetration of the perturbation depending on the plasma response is a complex issue [9, 10]. It is therefore interesting to investigate, whether a control of transport barrier relaxations can also be achieved with a single harmonic perturbation only, i.e. one island chain localized at one resonant surface and therefore no island overlap and no stochasticity. In the same framework, it is also important to study the possible mechanisms that can lead to an increase of the radial energy flux in presence of a magnetic island, as well as their relative importance.

In previous works, barrier relaxations have been studied by means of three-dimensional turbulence simulations [11, 12] and the possible control of these relaxations by externally induced
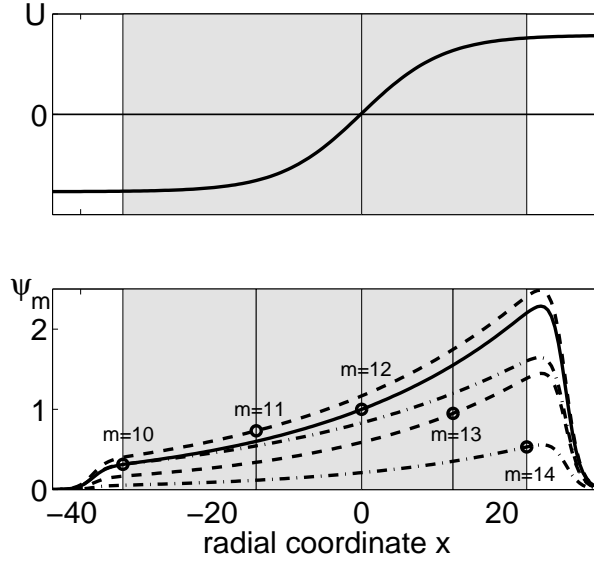
Figure 1: *Imposed rotation velocity U (top) and amplitudes ψ_m of the different harmonics of the prescribed poloidal magnetic flux perturbation (bottom), as a function of the normalized radial coordinate x. Circles indicate the amplitudes ψ_m on the corresponding resonant surfaces $q = m/n_0$.*

resonant magnetic perturbations has been investigated [13, 14]. In this framework, it has also been shown recently that a single harmonic resonant magnetic perturbation localized at the barrier position can also lead to a stabilization of the relaxations [15]. However, in this geometry, the confinement is always degraded.

As shown in these turbulence simulations, a key element for the stabilization of barrier relaxations is the convective energy flux associated with the non-axisymmetric plasma equilibrium in presence of magnetic islands. In fact, when a magnetic island chain is externally imposed inside the plasma, the modified equilibrium pressure and electric potential give rise to a convective flux that plays an important role in the local erosion of the transport barrier and the stabilization of its relaxations. The magnetic island chain can either result from a single harmonic resonant perturbation [15] or from a multiple harmonic resonant perturbation leading to a complex geometry with stochastic regions and residual islands [13, 14].

2. Turbulence model and transport barrier relaxations

2.1. Turbulence model

The three-dimensional turbulence model studied here consists of the normalized reduced MHD equations for the plasma pressure p and the electric potential ϕ [12],

$$\partial_t \nabla_\perp^2 \phi + \{\phi, \nabla_\perp^2 \phi\} \quad = -\nabla_\parallel^2 \phi - \mathbf{G}\, p + \nu \nabla_\perp^4 \phi + \mu \nabla_\perp^2 \left(\phi_{\mathrm{imp}} - \bar{\phi}\right) \; , \qquad (1)$$

$$\partial_t p + \{\phi, p\} \qquad = \delta_c \mathbf{G}\, \phi + \chi_\parallel \nabla_\parallel^2 p + \chi_\perp \nabla_\perp^2 p + S \; . \qquad (2)$$

In toroidal coordinates (r, θ, φ) and in a slab geometry (x, y, z) in the vicinity of a reference surface $r = r_0$ at the plasma edge, i.e. $x = (r - r_0)/\xi_{\mathrm{bal}}$, $y = r_0\theta/\xi_{\mathrm{bal}}$, $z = R_0\varphi/L_s$, the
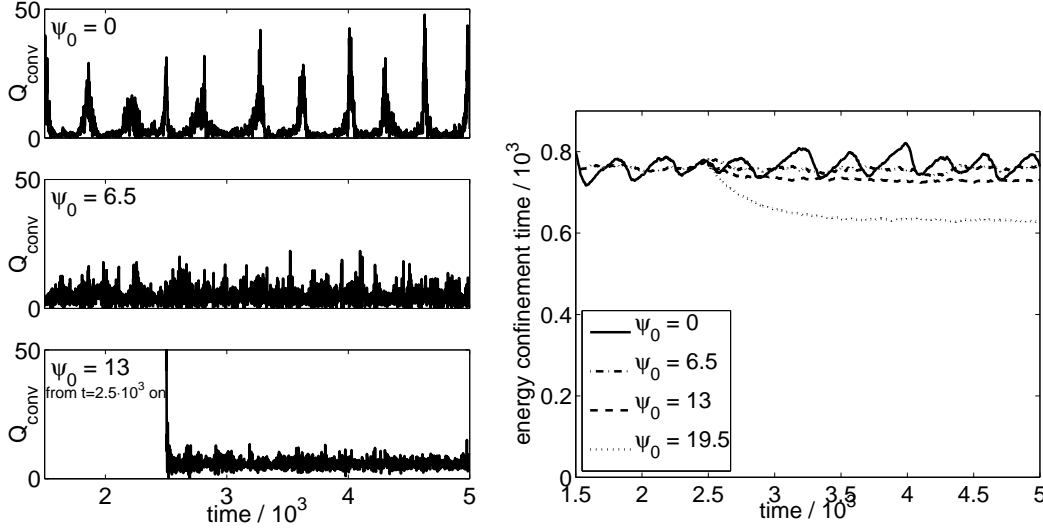
Figure 2: *Time evolutions of the convective flux* Q_{conv} *at the barrier center* $x = 0$, $q = 3$
(left) and of the edge energy confinement time $\tau_{E\,\text{edge}}$ *(right) for different amplitudes* ψ_0 *of the
multiple harmonics magnetic perturbation (5). Here,* $Q_{\text{tot}} = 10$, $\omega_{E\max} = 6$, $d = 11.7 =$
$0.15\,(x_{\max} - x_{\min})$.

normalized operators are

$$\nabla_\parallel = \partial_z + \left(\frac{\zeta}{q_0} - x\right)\partial_y - \{\psi_{\text{RMP}}, \,\cdot\,\} \quad \text{with} \quad \zeta = \frac{L_s r_0}{R_0 \xi_{\text{bal}}} \; ,$$

$$\mathbf{G} = \sin\theta\,\partial_x + \cos\theta\,\partial_y \; , \quad \nabla_\perp^2 = \partial_x^2 + \partial_y^2 \; , \quad \{\phi, \,\cdot\,\} = \partial_x\phi\partial_y - \partial_y\phi\partial_x \; ,$$

where ψ_{RMP} represents the externally imposed perturbation of the poloidal magnetic flux (see
section 3). Here, $q_0 = q(r_0)$ is the safety factor at the reference surface, R_0 is the major
radius of the magnetic axis and L_s is the shear length used as the scale length in the direction
parallel ($\parallel$) to the unperturbed magnetic field. The normalization length in the perpendicular
($\perp$) direction is the resistive ballooning length ξ_{bal} which for a collisional tokamak plasma
edge typically is of the order of ρ_s, the ion Larmor radius at electron temperature. Time is
normalized to the interchange time τ_{int} which typically is one order of magnitude larger than
the characteristic inverse drift frequency L_p/c_s, where c_s and L_p are the sound speed and
the pressure gradient length, respectively. Note that the perpendicular ion viscosity (ν) and
heat conductivity ($\chi_\perp$) coefficients in (1) and (2) are normalized using the perpendicular scale
length ξ_{bal}, whereas the parallel heat conductivity coefficient $\chi_\parallel$ is normalized with the parallel
scale length L_s. In the present simulations, we use $\nu = \chi_\perp = 0.93$ and $\chi_\parallel = 1$, and the ratio of
$\chi_\parallel/\chi_\perp \sim 1$ of the normalized coefficients corresponds to a ratio of the dimensional coefficients
of $L_s^2/\xi_{\text{bal}}^2 \sim 10^7 - 10^8$. Finally, $\delta_c = \frac{5}{3}2L_p/R_0$ is a curvature parameter set to $\delta_c = 0.01$.

In the present model, resistive ballooning turbulence is driven by an energy source S located
close to the inner boundary of the main computational domain. The latter corresponds to the
volume delimited by the toroidal surfaces characterized by $q = 2.5$ and $q = 3.5$, respectively,
and including the reference surface $q = q_0 = 3$. Here, a linear $1/q$ profile is assumed, and
$\xi_{\text{bal}}/r_0 = 1/500$, $L_s/R_0 = 1$. The complete computational domain is slightly larger and
delimited by $x_{\min} < x_{q=2.5}$ and $x_{\max} > x_{q=3.5}$. The source S gives rise to a constant incoming
(from the plasma center into the main computational domain) energy flux, $Q_{\text{tot}} = \int_{x_{\min}}^{x_{q=2.5}} S\,\mathrm{d}x$.
The pressure profile $\bar{p}(x,t) = \langle p\rangle_{y,z}$ evolves self consistently according to the energy transport
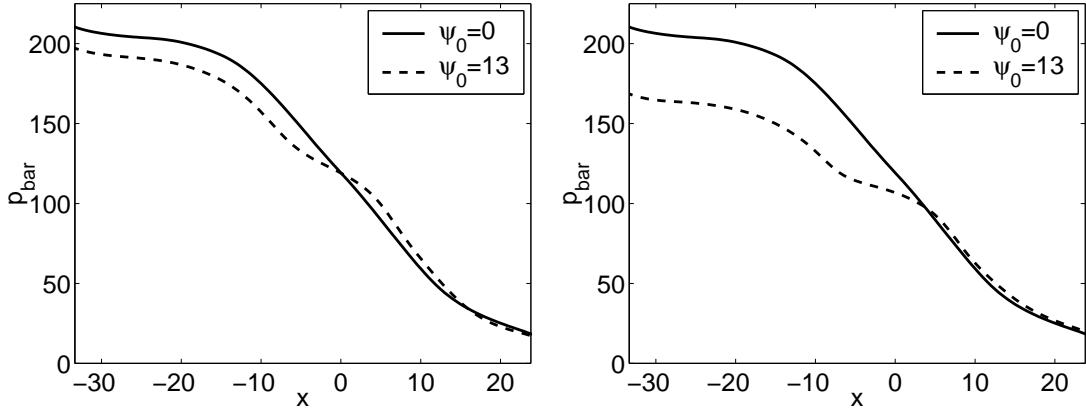
Figure 3: *Pressure profiles for different amplitudes ψ_0 of the multiple harmonics magnetic perturbation (5) (left) and the single harmonic magnetic perturbation (8) (right).*

equation [the toroidal and poloidal average $\langle \cdot \rangle_{yz}$ of (2)],

$$\partial_t \bar{p} = -\partial_x \left(Q_{\mathrm{conv}} + Q_{\mathrm{coll}} + Q_{\delta B} \right) + S \ , \tag{3}$$

with $Q_{\mathrm{conv}} = \langle p\,\partial_y\phi \rangle_{y,z}$, $Q_{\mathrm{coll}} = -\chi_\perp \partial_x \bar{p}$, $Q_{\delta B} = -\chi_\parallel \left\langle \partial_y \psi_{\mathrm{RMP}} \nabla_\parallel p \right\rangle_{y,z}$. In a statistically stationary state, averaging (3) in time and integrating in the radial direction leads to the energy flux balance

$$Q_{\mathrm{conv}}(x) + Q_{\mathrm{coll}}(x) + Q_{\delta B}(x) = Q_{\mathrm{tot}} \quad \text{for} \quad x \geq x_{\mathrm{q}=2.5} \ . \tag{4}$$

2.2 Transport barrier relaxations

When a poloidal $E \times B$ flow $U\mathrm{e}_y = \mathrm{d}_x\phi_{\mathrm{imp}}\mathrm{e}_y$ with radially localized velocity shear is imposed via an artificial friction term in (1) (with friction coefficient μ, and $\bar{\phi} = \langle \phi \rangle_{y,z}$), the turbulent radial energy flux Q_{conv} is reduced in the velocity shear region. According to the flux balance (4), when no magnetic perturbation is present ($\psi_{\mathrm{RMP}} = 0 \Rightarrow Q_{\delta B} = 0$), the pressure gradient steepens in the shear layer, i.e. a transport barrier forms [16]. Figure 1 (top) shows the profile of the rotation velocity $U = \omega_E d \tanh\left(x/d\right)$ used in the present simulations. The shear is maximal $\max\left(\mathrm{d}_x U\right) = \omega_E$ at the reference surface $q = 3$ leading to a transport barrier at that position. The parameter d characterizes the width of the velocity shear layer. Typically, such barrier is not stable but exhibits relaxation oscillations [11, 12]. Time traces of the convective flux Q_{conv} at the barrier center and the edge energy confinement time

$$\tau_{E\,\mathrm{edge}} = \frac{\int_{x_{q}=2.5}^{x_{q}=3.5} \bar{p}\,\mathrm{d}x}{Q_{\mathrm{tot}}}$$

are shown in Figure 2 (left, top) and (right), respectively. Quasi-periodic relaxations of the transport barrier are characterized by drops in the energy confinement time associated with strong flux peaks.

3. Effect of resonant magnetic perturbations on barrier dynamics
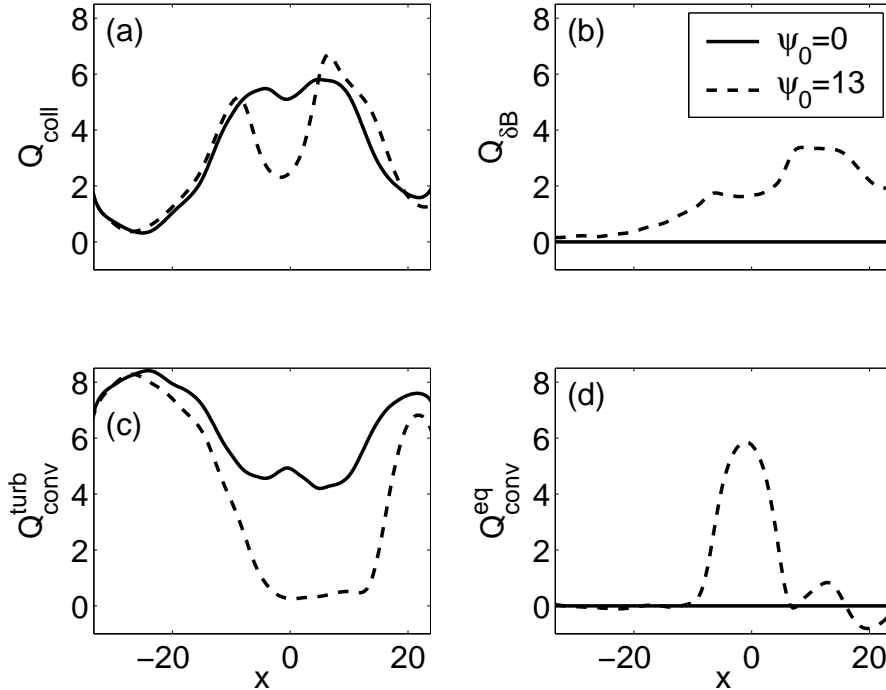
3.1. Multiple harmonics perturbation

Figure 4: *Radial profiles of the different contributions to the energy flux balance (4), with and without the multiple harmonics magnetic perturbation (5). According to (6) and (7), the convective flux is decomposed into two parts, one associated with the equilibrium and one associated with fluctuations. Parameters are the same as in Figure 2.*

In the electrostatic model (1), (2), we now impose a static resonant magnetic perturbation described by the normalized poloidal magnetic flux

$$\psi_{\mathrm{RMP}}^{\mathrm{multiple}} = \psi_0 \sum_m (-1)^m \psi_m(x) \cos\left(m\theta - n_0\varphi\right) \tag{5}$$

$$\text{with} \quad \psi_m(x) = C \frac{\sin\left[(m - m_0)\frac{\Delta\theta_c}{2\beta_1}\right]}{m(m - m_0)\pi} \exp\left[\frac{m}{\beta_1 r_c}\left(r_0 + \xi_{\mathrm{bal}}x - r_c\right)\right] \ .$$

Here, $(m_0, n_0) = (12, 4)$, $\Delta\theta_c = 2\pi/5$, $\beta_1 = 0.6$, and $r_c/\xi_{\mathrm{bal}} = 590$ are parameters typical for the DED device in the TEXTOR tokamak [17, 18] and the constant C is chosen such that $\psi_{m_0}(x = 0) = 1$. The radial profiles of the amplitudes $\psi_m(x)$ are shown in Figure 1 (bottom) for the five harmonics that are resonant in the main computational domain. Note that the amplitude of each harmonic m is increasing with radius but that the sizes of the magnetic islands induced by each harmonic m is determined by its amplitude at the corresponding resonant surface $q(x) = m/n_0$ (these amplitudes are indicated by circles in Figure 1).

For sufficiently high amplitudes ($\psi_0 \geq 6.5$), the perturbation (5) leads to a stabilization of the barrier relaxations [Figure 2 (left, middle and bottom)]. Except for very high perturbation amplitudes ($\psi_0 \geq 19$), the control of barrier relaxations is accompanied by only a slight degradation of the energy confinement time [Figure 2 (right)]. This behavior can be attributed to an erosion of the transport barrier and a steepening of the pressure gradient next to the barrier (on the outward side) [13, 14], as can be seen from Figures 3(left) and 4a.

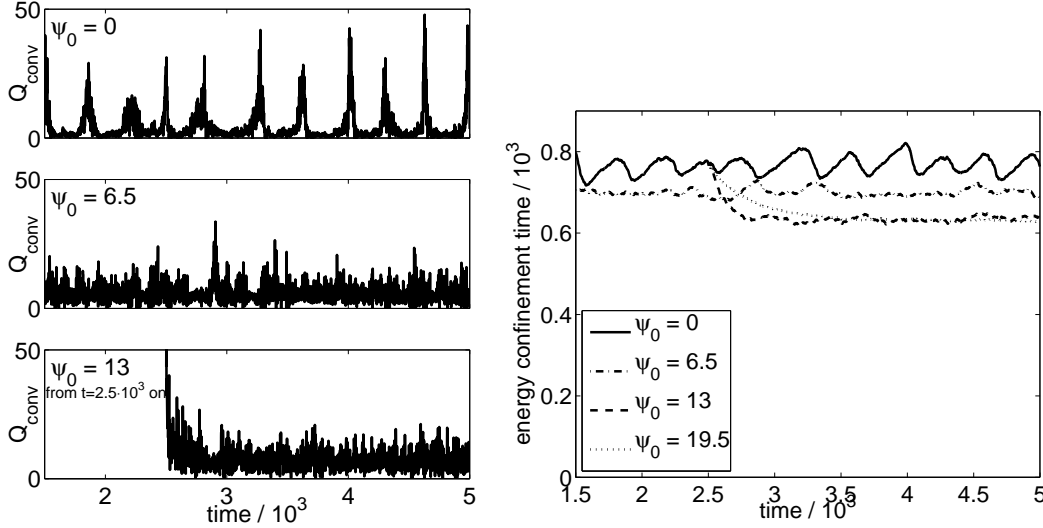Although the radial energy flux $Q_{\delta B}$, i.e. the radial component of the collisional parallel heat

Figure 5: *Time evolutions of the convective flux Q_{conv} at the barrier center $x = 0$, $q = 3$ (left) and of the edge energy confinement time $\tau_{E\,\mathrm{edge}}$ (right) for different amplitudes ψ_0 of the single harmonic magnetic perturbation (8). Parameters are the same as in Figure 2.*

flux on perturbed magnetic surfaces, is increasing with the perturbation amplitude ψ_0 (Figure 4b), the erosion of the transport barrier is mainly caused by the convective flux

$$Q_{\mathrm{conv}}^{\mathrm{eq}} = \langle p^{\mathrm{eq}} \partial_y \phi^{\mathrm{eq}} \rangle_{y,z} \tag{6}$$

associated with the non-axisymmetric plasma equilibrium in the presence of the magnetic perturbation. Here

$$p^{\mathrm{eq}}(x, y, z) = \langle p \rangle_t \ , \quad \phi^{\mathrm{eq}}(x, y, z) = \langle \phi \rangle_t \ ,$$

where $\langle \cdot \rangle_t$ is the time average in a statistically stationary state [19]. The convective energy flux associated with fluctuations,

$$Q_{\mathrm{conv}}^{\mathrm{turb}} = Q_{\mathrm{conv}} - Q_{\mathrm{conv}}^{\mathrm{eq}} \ , \tag{7}$$

is decreasing with the perturbation amplitude ψ_0 (Figure 4c), but the convective flux associated with the equilibrium Q_{conv}^{eq} is strongly increasing, especially in the barrier center (Figure 4d), where residual islands are present even for high perturbation amplitudes ψ_0 (when field line stochastisation occurs between the barrier and the outer plasma edge) [13, 14].

3.2. Single harmonic perturbation

As the stabilization of barrier relaxations is mainly due to an erosion of the barrier associated with a magnetic island chain localized at the barrier position, we expect a similar effect when restricting the perturbation (5) to the single harmonic that is resonant at $q = 3$,

$$\psi_{\mathrm{RMP}}^{\mathrm{single}} = \psi_0 \psi_{m_0}(x) \cos\left(m_0 \theta - n_0 \varphi\right) \quad \text{with} \quad \psi_{m_0}(x) = \exp\left(\frac{m_0 \xi_{\mathrm{bal}}}{\beta_1 r_c} x\right) \tag{8}$$

This magnetic perturbation is indeed stabilizing the barrier relaxations [Figure 5 (left, middle and bottom)], however, even for relatively low perturbation amplitudes ψ_0, this stabilization is accompanied by a significant reduction of the edge energy confinement time [Figure 5 (right)]. In fact, as shown in Figures 3(right) and 6a, the erosion at the barrier center is similar compared to the one observed with the multiple harmonics perturbation, but the single harmonic
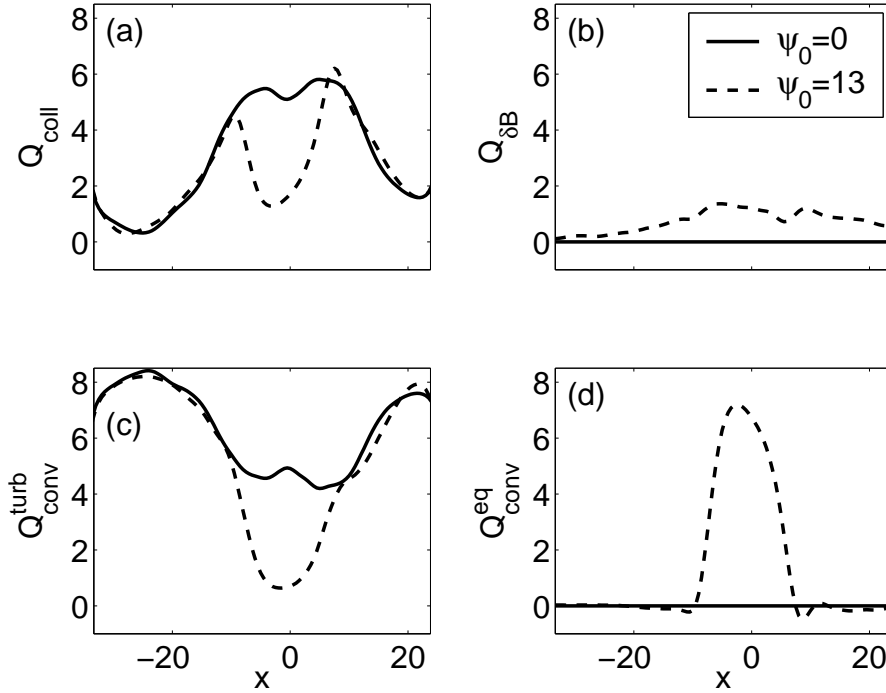
Figure 6: *Radial profiles of the different contributions to the energy flux balance (4), with and without the single harmonics magnetic perturbation (8). According to (6) and (7), the convective flux is decomposed into two parts, one associated with the equilibrium and one associated with fluctuations. Parameters are the same as in Figure 2. The island width corresponding to the perturbation amplitude $\psi_0 = 13$ is $W = 14.4$. We recall the shear layer width $d = 11.7$.*

perturbation does not affect the pressure profile far from its resonant surface. In particular, the steepening of the pressure gradient between the barrier and the outer edge, observed in the case of the multiple harmonics perturbation, and compensating for the erosion of the barrier, is not present in the case of the single harmonics perturbation [15]. In both cases, however, the erosion of the transport barrier is mainly due to the convective flux $Q_{\mathrm{conv}}^{\mathrm{eq}}$ associated with the helical plasma equilibrium induced by the magnetic island chain (Figures 4d and 6d).

4. Conclusions

Transport barrier relaxation oscillations observed in three-dimensional turbulence simulations can be controlled by multiple harmonics or single harmonic RMPs. This stabilization is due to an erosion of the barrier. In the first geometry, for intermediate perturbation amplitudes, the overall confinement is nearly unchanged because the erosion of the barrier is compensated by an increase of the pressure gradient outside the barrier. This steepening of the pressure gradient occurs in a layer where magnetic field lines stochasticity leads to a reduction of turbulent energy flux which is not completely compensated by the radial energy flux due to the collisional heat transport along perturbed magnetic field lines. Consequently, the single harmonics RMP always leads to a degradation of the confinement. The barrier erosion is due to an enhanced radial energy flux in the presence of magnetic islands. Two different mechanisms are at the origin of this enhancement. One is the radial energy flux due to the collisional heat transport along perturbed magnetic field lines. The second is a convective flux associated with the non-axisymmetric equilibrium in the presence of the magnetic island.

References.

[1] CONNOR, J.W., Plasma Phys. Control. Fusion **40**, 531 (1998).

[2] EVANS, T.E., et al., Phys. Rev. Lett. **92** 235003 (2004).

[3] BURRELL, K.H., et al., Plasma Phys. Control. Fusion **47** B37-B52 (2005).

[4] LIANG, Y., et al., Phys. Rev. Lett. **98** 265004 (2007).

[5] FINKEN, K.H., et al., Nucl. Fusion **47** 522 (2007).

[6] UNTERBERG, S.S., et al., J. Nucl. Mater. **390** 351 (2009).

[7] FITZPATRICK, R., Phys. Plasmas **2**, 825 (1994).

[8] BECOULET, M., et al., Nucl. Fusion **45** 1284 (2005).

[9] NARDON, E., BECOULET, M., HUYSMANS, G., and CZARNY, O., Phys. Plasmas **14**, 092501 (2007).

[10] BECOULET, M., et al., Nucl. Fusion **49** 085011 (2009).

[11] BEYER, P., BENKADDA, S., FUHR–CHAUDIER, G., et al., Phys. Rev. Lett. **94** 105001 (2005).

[12] BEYER, P., BENKADDA, S., FUHR–CHAUDIER, G., et al., Plasma Phys. Control. Fusion **49** 507 (2007).

[13] LECONTE, M., BEYER, P., GARBET, X., BENKADDA, S., Phys. Rev. Lett. **102** 045006 (2009).

[14] LECONTE, M., BEYER, P., GARBET, X., and BENKADDA, S., Nucl. Fus. **50** 054008 (2010).

[15] DE SOLMINIHAC, F., BEYER, P., LECONTE, M., et al., Contr. Plasma Phys. **50** 343 (2010).

[16] FIGARELLA, C.F., BENKADDA, S., BEYER, P., GARBET, X., VOITSEKHOVICH, I., Phys. Rev. Lett. **90** 015002 (1990).

[17] ABDULLAEV, S.S., FINKEN, K.H., JAKUBOWSKI M.W., KASILOV, S.V., KOBAYASHI, M., REISER, D., RUNOV, M.A., and WOLF, R., Nucl. Fusion **43** 299 (2003).

[18] HABERSCHEIDT, T., "Turbulenter Plasmatransport im ergodisierten Magnetfeld", PhD thesis, Univ. Bochum (2006)

[19] BEYER, P., GARBET, X., BENKADDA, S., GHENDRIH, P., SARAZIN, Y., Plasma Phys. Contr. Fusion **44** 2167 (2002).